


Robust Resource Allocation and Trajectory Planning of UAV-Aided Mobile Edge Computing in Post-Disaster Areas

Peng Cao ^{1,2}, Yi Liu ^{1,3,*} and Chao Yang ^{1,3} 

¹ School of Automation, Guangdong University of Technology, Guangzhou 510006, China; lhcaopeng_2010@163.com (C.P.); chyang513@gdut.edu.cn (C.Y.)

² Guangdong Key Laboratory of IoT Information Technology, Guangzhou 510006, China

³ Key Laboratory of Intelligent Detection and Internet of Manufacturing Things, Ministry of Education, Guangzhou 510006, China

* Correspondence: yi.liu@gdut.edu.cn

Abstract: When natural disasters strike, users in the disaster area may be isolated and unable to transmit disaster information to the outside due to the damage of communication facilities. Unmanned aerial vehicles can be exploited as mobile edge servers to provide emergency service for ground users due to its mobility and flexibility. In this paper, a robust UAV-aided wireless-powered mobile edge computing (MEC) system in post disaster areas is proposed, where the UAV provides charging and computing service for users in the disaster area. Considering the estimation error of users' locations, our target is to maximize the energy acquisition of each user by jointly optimizing the computing offloading process and the UAV trajectory. Due to the strongly coupled connection between optimization variables and the non-convex nature for trajectory optimization, the problem is difficult to solve. Furthermore, the semi-infinity of the users' possible location makes the problem even more intractable. To tackle these difficulties, we ignore the estimation error of users' location firstly, and propose an iterative algorithm by using Lagrange dual method and successive convex approximation (SCA) technology. Then, we propose a cutting-set method to deal with the uncertainty of users' location. In this method, we degrade the influence of location uncertainty by alternating between optimization step and pessimization step. Finally, simulation results show that the proposed robust algorithm can effectively improve the user energy acquisition.

Keywords: unmanned aerial vehicle; mobile edge computing; wireless power transfer; trajectory planning; robust design



Citation: Cao, P.; Liu, Y.; Yang, C. Robust Resource Allocation and Trajectory Planning of UAV-Aided Mobile Edge Computing in Post-Disaster Areas. *Appl. Sci.* **2022**, *12*, 2226. <https://doi.org/10.3390/app12042226>

Academic Editors: Andrzej Łukaszewicz and Yosoon Choi

Received: 24 January 2022

Accepted: 15 February 2022

Published: 21 February 2022

Publisher's Note: MDPI stays neutral with regard to jurisdictional claims in published maps and institutional affiliations.



Copyright: © 2022 by the authors. Licensee MDPI, Basel, Switzerland. This article is an open access article distributed under the terms and conditions of the Creative Commons Attribution (CC BY) license (<https://creativecommons.org/licenses/by/4.0/>).

1. Introduction

Natural disasters, such as earthquake, flood, and typhoon, often cause huge and unpredictable losses to human lives and properties [1–3]. Most of these disasters will result in unavailability of, or severe damage to, traditional terrestrial wireless infrastructures, as well as disruption to regional communication, which brings challenges to post-disaster response and relief [4–6]. By virtue of the advantages of dynamic mobility, flexibility, and on-demand deployment, unmanned aerial vehicles (UAVs) have been deemed as a promising technique in post-disaster area communication recovery [7–9]. In particular, the existence of line-of-sight (LoS) links between UAV and ground users has aroused a fast-growing interest in utilizing UAVs as aerial wireless platforms [10–13], while the limited power supply in disaster areas restricts the users' survival time and equipment performance, which also puts forward higher requirements for UAV-aided post-disaster services.

To tackle the above mentioned challenge, the combination of mobile edge computing (MEC) and wireless power transfer (WPT) seems to be an effective approach [14–16]. On one hand, by offloading computation tasks to UAVs, users can significantly improve their data processing capabilities [17–20]. On the other hand, with the aid of WPT technology, users can harvest radio-frequency (RF) signals from UAVs to prolong their survival time [21–23].

Unfortunately, the severe propagation loss of the wireless signals over long distances will degrade the performance of wireless information transfer (WIT) and WPT [24–26]. To improve the efficiency of WIT and WPT, UAVs should know the exact location of users in advance. However, in post-disaster areas, the exact location of users is difficult to obtain. The incomplete location information profoundly affects the trajectory planning of UAV and reduces the energy acquisition efficiency of users and the service quality of UAV [27–30]. Therefore, the robust design of trajectory and resource allocation of UAVs in post-disaster areas is of paramount importance.

Motivated by the requirements of a UAV-enabled wireless platform in a post-disaster area, we consider a robust UAV-enabled wireless-powered MEC system in this paper. In this system, a UAV equipped with MEC device and RF transmitter flies to the post-disaster area to provide computing and charging services for ground users. In this paper, we assume that terrestrial communications were destroyed in the disaster. Affected by this, the UAV only knows the rough areas where the users are, but the exact locations of the users are unknown. In order to ensure that users have enough power to maintain until the arrival of ground rescue, our target is to maximize the energy acquisition of each user while meeting the computation needs of users.

The considered problem is a non-convex semi-infinite optimization problem, which is intractable and hard to solve. In order to solve this intractability, we transform the original problem into a solvable form by ignoring the uncertainty of location first. Considering the coupling between computation offloading optimization and trajectory planning, an iterative optimization method is proposed by using Lagrange dual method and successive convex approximation (SCA) technology, respectively. Then, a cutting-set method is proposed to continuously decrease the impact of worst-case location of users on optimization. Due to the worst-case location of users changing with the optimization of UAV trajectory, the cutting-set method is achieved by alternating optimization, i.e., optimizing the UAV trajectory for given subsets of worst-case users' locations in the optimization step, and updating the subsets of worst-case users' locations according to UAV trajectory in the pessimization step.

To summarize, the difference between our work and those in [13,18] is mainly twofold. First, the proposed system considers the imperfect location information of users, which is more suitable for practical applications. Second, the proposed robust algorithm can effectively degrade the influence of location uncertainty on user energy acquisition. To our best knowledge, there are few studies that address the robust design for a UAV-enabled wireless-powered MEC system. In summary, the main contributions of this paper are as follows:

- We propose a UAV-enabled wireless-powered MEC system in a post-disaster area, while the imperfect location of users is considered. To ensure users have enough power in the post-disaster area, UAV provides charging and computing services for users.
- We propose a joint resource allocation and trajectory planning algorithm under known users' location to solve the strong coupling between optimization variables.
- We propose a robust cutting-set method to degrade the influence of worst-case location of users on optimization.

The rest of this paper is organized as follows. We describe the system model and formulate the optimization problem in Section 2. Then, we give a joint resource allocation and trajectory planning algorithm under known users' location in Section. In Section 4, we propose a robust cutting-set method. After this, the numerical results are presented in Section 5. Finally, we draw conclusions of our work in Section 6.

2. System Model and Problem Formulation

In this work, we propose a UAV-enabled wireless-powered MEC system in a post-disaster area, as shown in Figure 1. The terrestrial wireless infrastructures were damaged in the disaster. In order to get the situation of the disaster area and prepare for further rescue, a UAV, which is equipped with an RF transmitter and an MEC device, provides

charging and computing services for a set $\mathcal{N} \triangleq \{1, \dots, N\}$ of ground users, which has certain computation tasks R_n to complete, trapped in the disaster area.

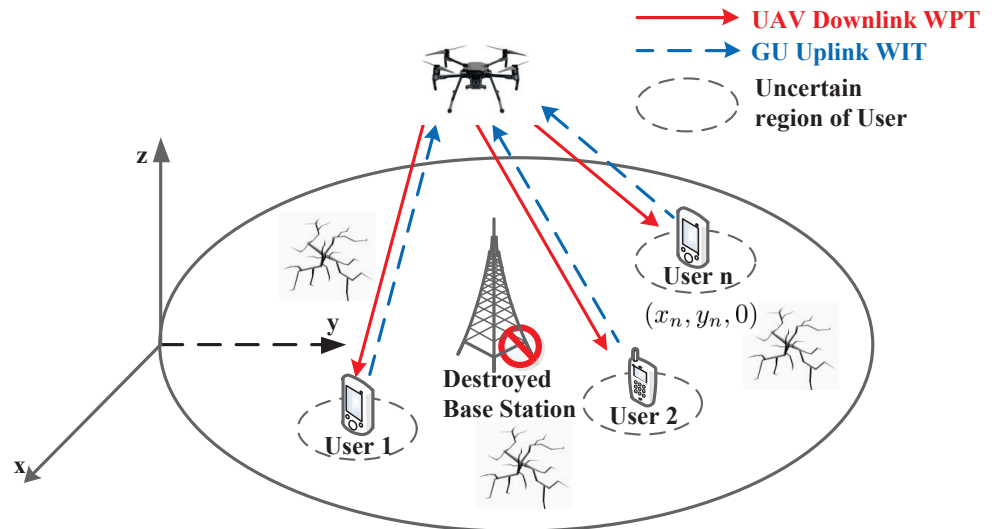


Figure 1. The UAV-enabled wireless-powered MEC system in post-disaster area.

Without loss of generality, we adopt a three-dimensional Euclidean coordinate system to represent the locations, and measure all dimensions in meters. Affected by the destruction of terrestrial wireless infrastructures, the UAV only knows the approximate location of n th users, denoted by $\mathbf{q}_n = (x_n, y_n, 0)$, with limited location information, while the exact location of n th users is $\bar{\mathbf{q}}_n = (\bar{x}_n, \bar{y}_n, 0)$, with a estimation error $\Delta\mathbf{q}_n$. The relation between the exact and approximate location of n th users is given by

$$\begin{aligned} \bar{\mathbf{q}}_n &= \mathbf{q}_n + \Delta\mathbf{q}_n, \\ \Delta\mathbf{q}_n &\in \Omega_n \triangleq \{\|\Delta\mathbf{q}_n\| \leq \varepsilon_n\}, \end{aligned} \tag{1}$$

where Ω_n is a continuous set of possible location estimation errors for the n th users, and ε_n denotes the radius of the uncertainly region Ω_n .

We assume that the UAV takes off and lands at a safe location $\mathbf{q}_s = (x_s, y_s, 0)$ within finite flight duration \mathcal{T} . The flight duration \mathcal{T} is discretized into T sufficiently small time slots with equal length $\delta = \mathcal{T}/T$. Thus, the UAV can be seen as fixed in a certain position in each time slot, and its horizontal plane coordinate at t th slot is $\mathbf{q}_u[t] = (x_t, y_t)$. Similar to [29], we assume that the UAV flies at a constant altitude H to avoid the flight energy consumption caused by frequent ascend or descend. Correspondingly, the distance between UAV and user n is

$$d_n[t] = \sqrt{H^2 + \|\mathbf{q}_u[t] - \mathbf{q}_n\|^2}, \tag{2}$$

where $\|\cdot\|$ denotes the Euclidean norm. Similar to [18], we assume the wireless channel between the UAV and users is LoS link. Then, the channel power gain between UAV and users is

$$g_n[t] = \beta_0 d_n[t]^{-2}, \tag{3}$$

where β_0 is the channel power gain at $d_0 = 1$ m.

In downlink WPT mode, we consider that the UAV uses constant transmission power P_u for wireless power transmission. The energy harvested by n th user is given as

$$E_h[t] = \eta g_n[t] P_u \delta, \tag{4}$$

where $0 < \eta \leq 1$ denotes the energy conversion efficiency of each user, while in uplink WIT mode, for given offloading power $P_{o,n}[t]$, the offloading rate $r_{tr,n}[t]$ of n th user in the t th slot is given as

$$r_{tr,n}[t] = B \log_2 \left(1 + \frac{P_{o,n}[t]g_n[t]}{\sigma^2} \right), \tag{5}$$

where B is the communication bandwidth, and σ^2 is the variance of additive white Gaussian noise with zero mean.

To utilize the energy in an efficient way, we assume that both UAV and users can adaptively adjust the CPU frequency [29]. The computation task amounts $R_{c,n}$ and the computation energy consumption $E_{c,n}$ of n th user in the t th slot are given as

$$\begin{aligned} R_{c,n} &= \frac{f_n[t]\delta}{C_n}, \\ E_{c,n} &= \theta_n f_n[t]^3 \delta, \end{aligned} \tag{6}$$

where $f_n[t]$ represents the CPU frequency of users, C_n denotes the number of CPU cycles to complete the computation, and θ_n is the effective capacitance coefficient of the CPU. The expressions of computation amounts $R_{c,u}$ and computation energy consumption $E_{c,u}$ of UAV are consistent with users, which are not listed here.

For given UAV trajectory, we can obtain the flight speed of UAV on the horizontal plane:

$$v_u(t) = \frac{\|\mathbf{q}_{u,t+1} - \mathbf{q}_{u,t}\|}{\delta}. \tag{7}$$

For safety consideration, the maximum flight speed of UAV is v_{max} . In order to focus on designing the robust algorithm of trajectory planning and computation offloading optimization, we adopt a simplified flight energy consumption model in this work, while many factors will affect the flight energy consumption of UAV in reality. The flight energy consumption of UAV can be expressed as

$$E_{fly}[t] = 0.5m_u \delta v_u[t]^2, \tag{8}$$

where m_u is the mass of UAV.

Considering the inconvenience of obtaining energy in post-disaster areas, it is necessary for users to obtain charging and computing services from UAVs as much as possible to ensure that users gain more energy. The energy gain of the n th user is given as

$$E_{gain,n} = \sum_{t=1}^T (\eta g_n[t] P_u - \theta_n f_n[t]^3) - \sum_{t=1}^{T-1} P_{o,n}[t]. \tag{9}$$

In this work, our target is to maximize the minimum energy gain among users while guaranteeing the completion of computation task; the UAV trajectory and offloading optimization variables are jointly optimized under the estimation error of users' location. Then, the optimization problem can be formulated as

$$\mathbf{P1} : \max_{\Theta} \min_{n \in \mathcal{N}} \max_{\Delta \mathbf{q}_n \in \Omega_n} E_{gain,n}, \tag{10a}$$

$$s.t. \quad C1 : \sum_{t=1}^T (E_{fly}[t] + P_u) + \sum_{t=2}^T \theta_u f_u[t]^3 \leq E_{bat}, \tag{10b}$$

$$C2 : \sum_{t=1}^T \frac{f_n[t]}{C_n} + \sum_{t=1}^{T-1} r_{tr,n}[t] \geq R_n, \forall n \in \mathcal{N}, \tag{10c}$$

$$C3 : \sum_{t=2}^T \frac{f_u[t]}{C_u} \geq \sum_{n=1}^N \sum_{t=1}^{T-1} r_{tr,n}[t], \forall t \in \mathcal{T}, \tag{10d}$$

$$C4 : f_u[t] \geq 0, f_n[t] \geq 0, \forall n \in \mathcal{N}, \tag{10e}$$

$$C5 : \mathbf{q}_u[1] = \mathbf{q}_u[T+1] = \mathbf{q}_s, \tag{10f}$$

$$C6 : v_u[t] \leq v_{max}, \forall t \in \mathcal{T}. \tag{10g}$$

where $\Theta = \{\mathbf{q}_u[t], f_u[t], f_n[t], P_{o,n}[t]\}$ is the optimal variable set, and \mathcal{T}_{-T} represents the set \mathcal{T} except the T th time slot. C1 is the UAV battery constraint; C2 represents all computation tasks for each user need to be processed; C3 denotes that all computation task from users should to be handled by UAV in time; C4 are the CPU frequency constraints of user and UAV; C5 indicates that the UAV takes off and lands at the same safe position; C6 gives the maximum flight speed constraint of UAV.

3. Joint Resource Allocation and Trajectory Planning under Known Users' Location

In this section, we propose a joint resource allocation and trajectory planning algorithm to solve problem **P1** under known users' location. For the known users' location, we can ignore the estimation error ε_n of users, i.e., let $\hat{\mathbf{q}}_n := \mathbf{q}_n, \forall n \in \mathcal{N}$. Then, the original optimization problem **P1** can be transformed to

$$\mathbf{P2} : \max_{\Theta} \min_{n \in \mathcal{N}} \hat{E}_{gain,n}, \tag{11a}$$

$$s.t. \quad C1 - C6. \tag{11b}$$

Due to the coupling among the optimization variables, **P2** is still difficult to solve. Thus, we divide the optimization problem into two parts, i.e., computation offloading optimization and trajectory planning, and optimize them alternately. Firstly, we optimize the computation offloading resources by Lagrangian duality method under given UAV trajectory. Then, the SCA method is adopted to optimize the UAV trajectory for given computation offloading resources.

3.1. Computation Offloading Optimization

For given UAV trajectory, we can obtain the computation offloading variables optimization problem **P3**:

$$\mathbf{P3} : \min_{P_{o,n}, f_u, f_n} \sum_{t=1}^T \theta_n f_n[t]^3 + \sum_{t=1}^{T-1} P_{o,n}[t], \tag{12}$$

$$s.t. \quad C2, C4.$$

Obviously, **P3** is a convex problem, which can be easily solved by Lagrange duality method. Then, we can obtain Theorem 1 by solving the Lagrangian function.

Theorem 1. For given UAV trajectory $\mathbf{q}_u(t)$, the optimal offloading power and CPU frequencies of users can be respectively expressed as

$$P_{o,n}^{opt}[t] = \left[\frac{\lambda B}{\ln 2} - \frac{\sigma^2}{g_n[t]} \right]^+, \tag{13}$$

$$f_n^{opt}[t] = \sqrt{\frac{\lambda}{3\theta_n C_n}}, \tag{14}$$

where $\lambda \geq 0$ denotes the dual variable associated with the constraint C2.

Proof. See the Appendix A. \square

Then, we adopt the subgradient method to obtain the value of dual variables.

$$\lambda(i + 1) = [\lambda(i) - \theta(i)\Delta\lambda(i)]^+, \tag{15}$$

where i represents the iteration index, $\theta(i)$ denotes the iterative step, and the corresponding subgradient $\Delta\lambda(i)$ can be obtained by

$$\Delta\lambda(i) = \sum_{t=1}^T \frac{f_n^{i,opt}[t]}{C_n} + \sum_{t=1}^{T-1} B \log_2 \left(1 + \frac{P_{o,n}^{i,opt}[t]g_n[t]}{\sigma^2} \right) - R_n, \tag{16}$$

where $f_n^{i,opt}[n]$, $P_{o,n}^{i,opt}[t]$ represent the optimal solutions at the i th iteration.

Then, according to optimal offloading power $P_{o,n}^{i,opt}[t]$ and constraint C3, we can obtain the optimal CPU frequencies of UAV

$$f_u^{i,opt}[t] = \frac{B}{\delta} \sum_{n=1}^N \log_2 \left(1 + \frac{P_{o,n}^{i,opt}[t]g_n[t]}{\sigma^2} \right), \tag{17}$$

since the lowest computation energy consumption can be obtained only when the computation frequency is a constant.

3.2. UAV's Trajectory Planning

For given computation offloading variables, the UAV's trajectory optimization problem **P4** can be expressed as

$$\begin{aligned} \mathbf{P4} : \quad & \max_{\mathbf{q}_u[t]} \min_{n \in \mathcal{N}} \sum_{t=1}^T \eta g_n[t] P_u \\ & \text{s.t.} \quad \text{C1, C2, C5, C6.} \end{aligned} \tag{18}$$

Due to the objective function of **P4** being non-concave and the constraint C2 being non-convex with respect to $\mathbf{q}_u[t]$, the problem **P4** is non-convex. For this problem, we choose the SCA method to solve.

By adopting the SCA method, we can obtain

$$\begin{aligned} r_{tr,n}[t] \geq r_{tr,n}^{low} = & B \log_2 \left(1 + \frac{P_{o,n}[t]\beta_0}{\sigma^2(H^2 + l_n^j[t]^2)} \right) \\ & - \frac{P_{o,n}[t]\beta_0 \log_2 e (l_n[t]^2 - l_n^j[t]^2)}{(H^2 + l_n^j[t]^2)(\sigma^2 H^2 + \sigma^2 l_n^j[t]^2 + P_{o,n}[t]\beta_0)}, \end{aligned} \tag{19}$$

where $l_n[t] = \|\mathbf{q}_u[t] - \mathbf{q}_n\|$, the r_k^{low} is the lower bound of $r_n[t]$, and the equality holds when $l_n[t] = l_n^j[t]$.

Similarly, we can obtain the lower bound g_n^{low} of $g_n[t]$:

$$g_n[t] \geq g_n^{low} = \frac{\beta_0(H^2 + 2l_n^j[t]^2 - l_n[t]^2)}{(H^2 + l_n^j[t]^2)^2}. \tag{20}$$

According to Formulas (19) and (20), we can transform the problem **P4** to

$$\mathbf{P4.1} : \max_{\mathbf{q}_u[t]} \sum_{t=1}^N \eta g_n^{low} P_u \tag{21a}$$

$$\text{s.t. C2.1 : } \sum_{t=1}^T \frac{f_n[t]}{C_n} + \sum_{t=1}^{T-1} r_{tr,n}^{low} \geq R_n, \forall n \in N, \tag{21b}$$

$$\text{C1, C5, C6.} \tag{21c}$$

In problem **P4.1**, we can find that the objective function and the constraint C2.1 are both convex with respect to $\mathbf{q}_u[t]$. Thus, the problem **P4.1** is a convex problem. We can use CVX to solve this problem.

3.3. Alternative Algorithm for Solving P2

Based on the Lagrangian duality method and SCA method, we propose a joint resource allocation and trajectory planning (JRATP) algorithm under known users' location in this subsection. The detailed JRATP algorithm is shown in Algorithm 1.

Algorithm 1 Joint Resource Allocation and Trajectory Planning Algorithm under known users' location

Input: Initialize $P_{o,n}^1[t], f_n^1[t], f_u^1[t], \mathbf{q}_u^1[t]$ with feasible solution.

Initialization: Set the radio environment parameters B, β_0, σ^2 , the operation parameters $P_u, \eta, C_n, C_u, \theta_n, \theta_u$, and the tolerance error $\varepsilon_1, \varepsilon_2$

For each iteration i

Calculate $P_{o,n}^{i,opt}[t], f_n^{i,opt}[t]$ by Theorem 1 and calculate $f_u^{i,opt}[t]$ according to (17);

Update $\Delta\mu(i)$, and $\mu(i+1)$ by subgradient formula;

$P_{o,n}^{i+1}[t] = P_{o,n}^{i,opt}[t], f_n^{i+1}[t] = f_n^{i,opt}[t], f_u^{i+1}[t] = f_u^{i,opt}[t], q_u^j[t] = q_u^i[t]$.

For each iteration j

Using CVX to solve **P4.1** for given $P_{o,n}^{opt,j}[t], f_n^{opt,j}[t], f_u^{opt,j}[t]$ and obtain $\mathbf{q}_u^{opt,i}[t]$;

If $\sum_{t=1}^N \|\mathbf{q}_u^{j+1}[t] - \mathbf{q}_u^j[t]\| \leq \varepsilon_2, \mathbf{q}_u^i[t] = \mathbf{q}_u^j[t]$, **break**

End If

update $j = j + 1$;

End For

If $\|\sum_{t=1}^T (R_{c,n}^i[t] - R_{c,n}^{i-1}[t]) + \sum_{t=1}^{T-1} (R_{o,n}^i[t] - R_{o,n}^{i-1}[t])\| \leq \varepsilon_1$, **break**

End If

update $i = i + 1$;

End For

Output $P_{o,n}^{opt}[t], f_n^{opt}[t], f_u^{opt}[t], \mathbf{q}_u^{opt}[t]$.

The complexity of Algorithm 1 comes from three aspects: (1) the computation of offloading power and CPU frequencies, (2) the computation of the dual variables, and (3) the application of CVX for computing UAV trajectory. Let L_1 and L_2 denote the number of iterations required for the outer loop and the inner loop of Algorithm 1. Let ϕ denote the tolerance error for the subgradient method. Then, we can obtain the total complexity of Algorithm 1 as $\mathcal{O}[L_1(2NT + 1/\phi^2 + L_2T^3)]$, where $\mathcal{O}(\cdot)$ is the big-O notation.

By solving each subproblem alternately, Algorithm 1 can guarantee convergence, while, due to the usage of SCA method and alternating optimization, the global optimum of problem **P2** cannot be strictly guaranteed.

4. Robust Design Based on Cutting-Set Method

In this section, we give a cutting-set method to degrade the influence from the uncertainty of the users' locations. The robust design is achieved by alternating between optimization steps and pessimization steps. In the optimization step, joint resource allocation and trajectory planning are optimized under a given finite subset of worst-case users' locations by Algorithm 1. Then, in the pessimization step, the subset of worst-case users' locations is updated according to the UAV trajectory obtained in the optimization step.

4.1. Optimization Step under Finite Subsets of Users' Location

Note that the worst-case locations of users are changed with the change of UAV trajectory in the optimization process. To simplify the problem, we assume that the worst-case locations of users are included in a finite subset of potential locations. Let \mathcal{S}_n denote the potential worst-case locations of the n th user. Then, we can express the finite subset of the n th user in the k th optimization as $\mathcal{S}_n^k \subset \mathcal{S}_n$. For a given finite subset, we can transform the original problem to

$$\begin{aligned} \mathbf{P5} : \quad & \max_{\Theta} \min_{n \in \mathcal{N}} \max_{\mathbf{q}_n \in \mathcal{S}_n^k} E_{gain,n} \\ \text{s.t.} \quad & \text{C1} - \text{C6}, \end{aligned} \tag{22}$$

while the problem **P5** can be solved by Algorithm 1.

4.2. Pessimization Step under Given UAV Trajectory

For a given UAV trajectory obtained from the optimization step, the worst-case users' location is updated in this step. Considering that the distances $d_n[t]$ between the UAV and users are larger than the estimation error $\Delta \mathbf{q}_n$, in the optimization process, we discretize the potential locations of the n th user into equal spacing grids-based worst-case locations with the resolution of π .

For the UAV, the worst-case locations under different trajectories is also different. Thus, the worst-case users' location needs to be updated after each trajectory planning, while, for the users, the location with the least energy harvest and the most transmission energy consumption corresponds to the worst-case location. Thus, the worst-case location $\mathbf{q}_n^{w,k}$ of n th user after k th optimization is obtained as

$$\|\mathbf{q}_u - \mathbf{q}_n^{w,k}\| = \|\mathbf{q}_n - \mathbf{q}_n^{w,k}\| + \varepsilon_n. \tag{23}$$

Then, the obtained worst-case locations $\mathbf{q}_n^{w,k}$ of the n th user is added into the infinite subset \mathcal{S}_n^k for the next turn of optimization.

4.3. Total Algorithm of Robust Resource Allocation and Trajectory Planning

Based on the cutting-set method, we propose a robust resource allocation and trajectory planning algorithm to solve the uncertainty of users' location in this subsection. The detailed robust algorithm is shown in Algorithm 2.

As shown in Algorithm 2, the finite subset of potential users' locations are firstly initialized. Firstly, for a given finite subset of users' locations, the optimal computation offloading variables $P_{o,n}^k[t]$, $f_n^k[t]$, $f_u^k[t]$ and UAV trajectory $\mathbf{q}_u^k[t]$ are obtained by solving **P5** with Algorithm 1. Then, based on the UAV trajectory from the previous step, we can obtain the worst-case users' location and add it into \mathcal{S}_n^k for the next turn of optimization. The robust algorithm processes alternately until the improvement reaches the stable point or reaches the maximum number k of iterations.

Algorithm 2 Robust Offloading Trajectory and Computation Offloading Algorithm with uncertainty of users' location

Initialization: Set the iterative number $k = 1$.
Input: Initialize finite subset \mathcal{S}_n^k .
repeat
 calculate $P_{o,n}^k[t], f_n^k[t], f_u^k[t]$ and $\mathbf{q}_u^k[t]$ by Algorithm 1;
 compute $\mathbf{q}_n^{w,k}$ for given $\mathbf{q}_u^k[t]$;
 update finite subset $\mathcal{S}_n^{k+1} = \{\mathcal{S}_n^k, \mathbf{q}_n^{w,k}\}$;
 update $k = k + 1$;
until reach the stable point or the maximum iterative number k
Output $P_{o,n}^k[t], f_n^k[t], f_u^k[t], \mathbf{q}_u^k[t]$.

5. Numerical Results

In this section, simulation results are presented to validate the performance of the proposed robust joint resource allocation and trajectory planning algorithm, and are compared with three benchmark schemes. (1) Non-robust: In this scheme, we ignore the estimation error and optimize the problem under the estimated locations. (2) No-resource-allocation-optimization: In this scheme, we offload all computation tasks to UAV with fixed offloading power $P_{o,n} = P_{o,max}$. (3) No-trajectory-planning: In this scheme, we set the UAV trajectory as a circle around users with a radius 200 m.

According to the parameters adopted in [21,30], we consider a 500×500 m² post-disaster area which includes five ground users. The location estimation errors of the users are $\epsilon_n = 20$ m. The flight altitude of UAV is $H = 50$ m, and the maximum flight speed of UAV is set as $V_{max} = 25$ m/s. The detailed environment settings are given in Table 1.

Table 1. Simulation parameters.

B	5 MHz	The channel bandwidth.
β_0	−50 dB	The channel power gain at distance $d_0 = 1$ m.
σ^2	10^{-9} W	The receiver noise power.
$P_{o,n}^{max}$	0.5 W	The maximum WIT transmit power of user.
P_u	50 W	The WPT transmit power of UAV.
η	0.15	The energy conversion efficiency of user.
C_n, C_u	10^3 cycles/bit	The number of CPU cycles.
θ_n, θ_u	10^{-28}	The effective switched capacitance.
$f_{n,max}, f_{u,max}$	10 GHz	The maximum frequency of CPU.

In Figure 2, we present the optimized UAV trajectories of the proposed robust joint resource allocation and trajectory planning algorithm and non-robust scheme under different battery capacity. From Figure 2, we can find that with the increase of battery capacity, the UAV can approach each user to provide services. The reason is that on the premise of completing the computation task, the larger the UAV battery capacity, the closer it can be to the users to provide efficient charging services. Note that under the same battery capacity, the proposed robust algorithm is much closer to users than the non-robust scheme. This is because in order to eliminate the impact of the worst-case location error on the users' power supply, the UAV should be close to the user greatly affected by the location error.

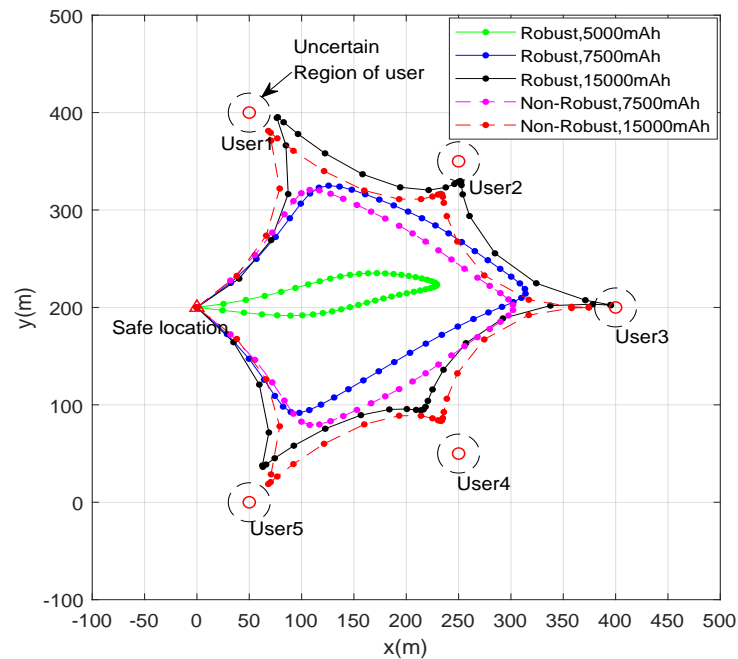


Figure 2. The optimized UAV trajectories under different schemes and battery capacity.

Figure 3 shows the minimum energy gain of users of the proposed robust algorithm with the other three benchmark schemes with different battery capacity of UAV. According to Figure 3, we can find that the proposed robust algorithm obtains the highest energy gain compared with other schemes. The reason is that the proposed robust algorithm can maximize the minimum energy gain of users by jointly optimizing UAV's trajectory and offloading process, and decreasing the influence of estimation location errors, while the other three schemes only optimize two of the three variables. We can also observe that with the increase of battery capacity, the energy gain of users increases rapidly, and then slows down gradually. That is, a larger UAV battery capacity can ensure UAV approach to users to provide much more efficient charging services. As the distance between UAV and users decreases, the impact of distance on energy supply decreases gradually, which leads to the slowing down of energy gain. In addition, the energy gain of the no-trajectory-planning scheme is a constant when battery capacity is bigger than 11,000 mAh. The reason is that when the battery capacity can ensure that the UAV flies according to the fixed trajectory, the distance between UAV and user is a constant. Then, the increase of battery capacity will not affect the energy gain of users.

In Figure 4, we compare the minimum energy gain of users of the proposed robust algorithm with the other three benchmark schemes with different estimation errors of users. From Figure 4, we can find that with the increase of the estimation errors, the minimum energy gain is decreased, while the reduction of the proposed robust algorithm is less than the non-robust scheme and the no-trajectory-planning scheme. This is because with the increase of the estimation errors, the worst-case location error will greatly increase the distance between UAV and user. Furthermore, compared with the no-trajectory-planning scheme flying as a circle, the non-robust scheme has less time to approach the user, which also leads to the fastest decline among all the schemes. Therefore, for the environment with location errors, it is necessary to introduce robust design into trajectory optimization.

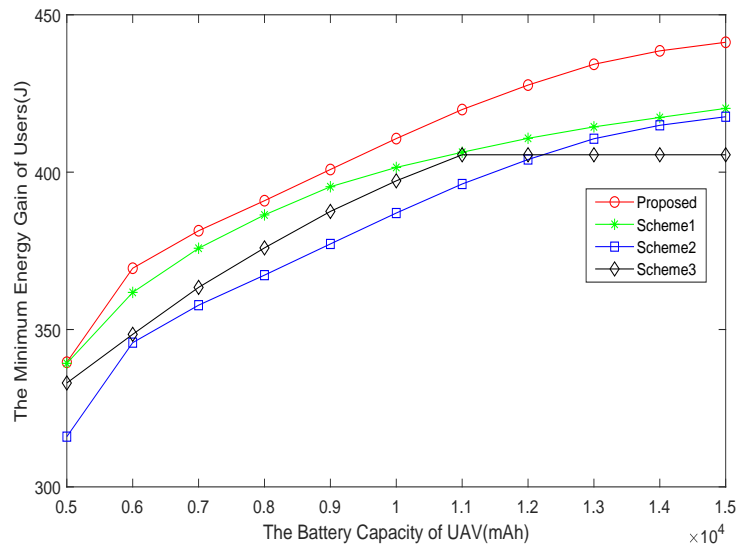


Figure 3. Energy gain of users under different schemes and battery capacity of UAV.

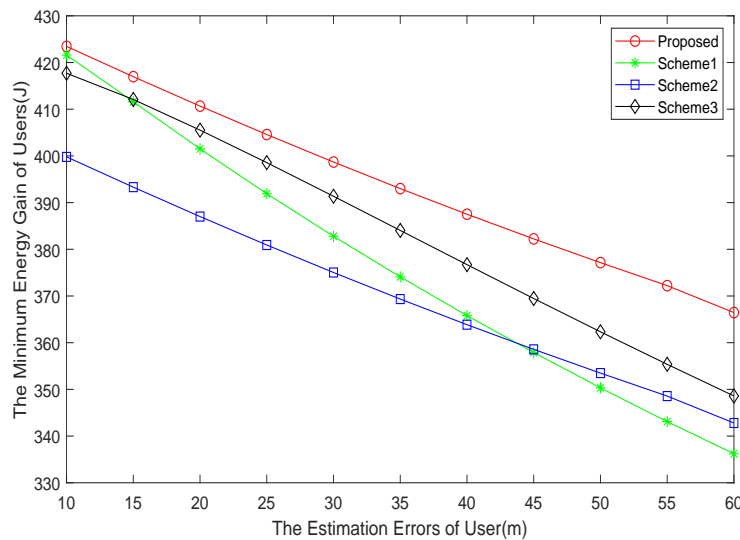


Figure 4. Energy gain of users under different schemes and estimation errors of users.

The distance between UAV and user is affected by horizontal distance and flight altitude. Thus, we present the minimum energy gain of users of the proposed robust algorithm with the other three benchmark schemes with different flight altitude of UAV in Figure 5. It can be seen that with the increase of flight altitude, the decrease of user energy gradually speeds up. The reason is that when the flight altitude is greater than the horizontal distance $d_n[t]$, the distance between the UAV and users is mainly affected by the flight altitude, and vice versa. Thus, in order to ensure that users receive more energy, the UAV can appropriately reduce the flight altitude when the estimation error is small.

Figure 6 also compares the minimum energy gain of users of the proposed robust algorithm with the other three benchmark schemes with different WPT transmit power of UAV. We can find that the energy gain achieved by the proposed robust algorithm is the highest among the schemes, while the increase of energy is proportional to the transmission power. That is, the user’s energy gain is only affected by the transmitting power of the UAV when the computation task is processed.

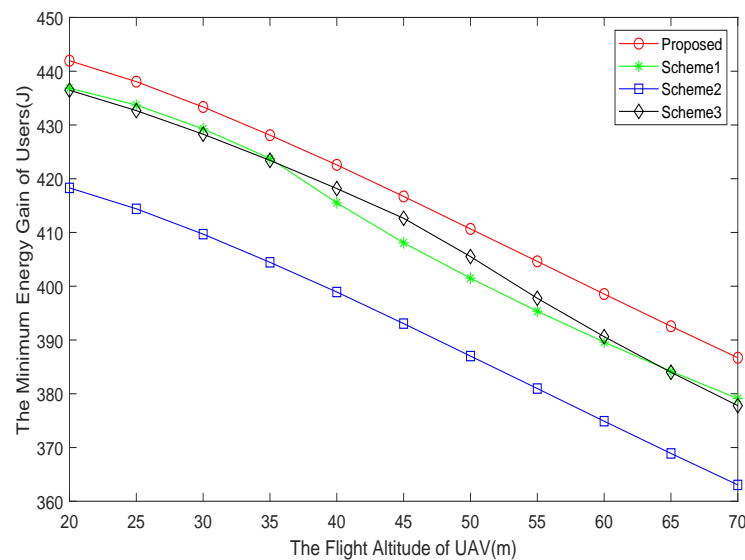


Figure 5. Energy gain of users under different schemes and flight altitude of UAV.

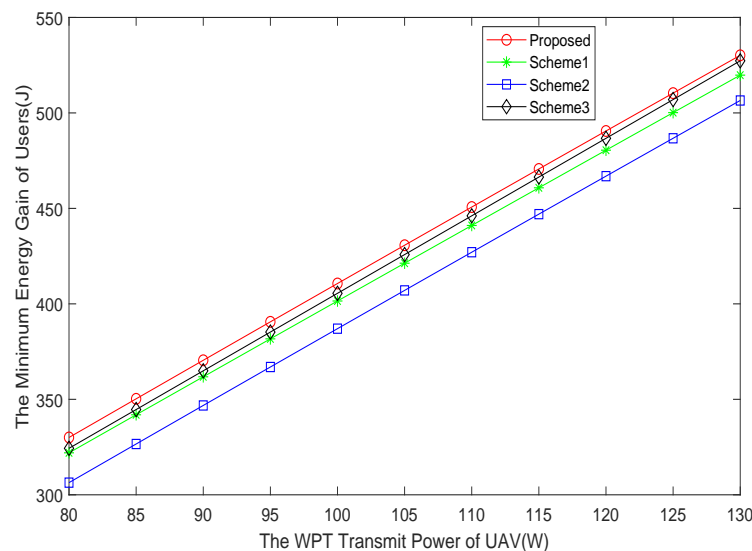


Figure 6. Energy gain of users under different schemes and WPT transmit power of UAV.

6. Conclusions

In this paper, we proposed a robust UAV-aided wireless-powered MEC system in a post-disaster area, where the UAV provides charging and computing services for ground users to ensure that users have enough power. To maximize the energy acquisition of each user, we jointly optimized the computing offloading and UAV trajectory. Particularly due to the destruction of terrestrial communications, the UAV only has an imperfect location of the users. Considering the strongly coupled connection between optimization variables and the influence of user location estimation error, the robust resource allocation and trajectory planning was carefully addressed. Firstly, we proposed a joint resource allocation and trajectory planning algorithm under known users' location. Then, the robust cutting-set method was proposed to reduce the impact of worst-case location of users on optimization. Finally, we conducted extensive simulations to verify the effectiveness of the proposed robust algorithm.

Author Contributions: Conceptualization, P.C. and Y.L.; methodology, P.C. and Y.L.; software, P.C. and Y.L.; validation, Y.L. and C.Y.; formal analysis, P.C.; investigation, P.C.; resources, P.C.; data curation, P.C. and C.Y.; writing—original draft preparation, P.C. and C.Y.; writing—review and

editing, Y.L. and C.Y.; visualization, C.Y.; supervision, Y.L. and C.Y.; project administration, Y.L.; funding acquisition, Y.L. All authors have read and agreed to the published version of the manuscript.

Funding: This work was supported in part by the National National Key R&D Program of China under Grants 2020YFB1807805, 2020YFB1807800; in part by the Guangdong Basic and Applied Basic Research foundation under Grant 2019A151501114.

Institutional Review Board Statement: Not applicable.

Informed Consent Statement: Not applicable.

Data Availability Statement: Not applicable.

Conflicts of Interest: Not applicable.

Abbreviations

The following abbreviations are used in this manuscript:

UAV	Unmanned aerial vehicle
MEC	Mobile edge computing
WPT	Wireless power transfer
WIT	Wireless information transfer
RF	Radio frequency
SCA	Successive convex approximation

Appendix A

Proof of Theorem 1. Let $\lambda \geq 0$ denotes the dual variable associated with the constraint C2. Then, for each user, we can get the Lagrangian function of \mathbf{P}_{4-1} as

$$\mathcal{L}(\Theta) = \sum_{t=1}^T (\eta g_n[t] P_u - \theta_n f_n[t]^3) - \sum_{t=1}^{T-1} P_{o,n}[t] + \lambda \left\{ \sum_{t=1}^T \frac{f_n[t]}{C_n} + \sum_{t=1}^{T-1} r_{tr,n}[t] - R_n \right\}.$$

Taking the derivative of the Lagrangian function \mathcal{L} w.r.t CPU frequency $f[n]$ and offloading power $P_{o,n}[t]$ yields

$$\begin{aligned} \frac{\partial \mathcal{L}(\Theta)}{\partial P_{o,n}[t]} &= \lambda \frac{B}{\ln 2} \frac{\tilde{g}_n[t]}{\sigma^2 + P_{o,n}[t] \tilde{g}_n[t]} - 1, \\ \frac{\partial \mathcal{L}(\Theta)}{\partial f_n[t]} &= -3\theta_n f_n[t]^2 + \frac{\lambda}{C_n}. \end{aligned}$$

Let $\frac{\partial \mathcal{L}}{\partial P_{o,n}[t]} = 0$ and $\frac{\partial \mathcal{L}}{\partial f_n[t]} = 0$, the optimal $P_{o,n}^{opt}[t]$ and $f_n^{opt}[t]$ can be obtained. The proof of Theorem 1 is finished. \square

References

1. Erdelj, M.; Natalizio, E.; Chowdhury, K.R.; Akyildiz, I.F. Help from the Sky: Leveraging UAVs for Disaster Management. *IEEE Pervasive Comput.* **2017**, *16*, 24–32. [\[CrossRef\]](#)
2. Yao, Z.; Cheng, W.; Zhang, W.; Zhang, H. Resource Allocation for 5G-UAV-Based Emergency Wireless Communications. *IEEE J. Sel. Areas Commun.* **2021**, *39*, 3395–3410. [\[CrossRef\]](#)
3. Chen, W.; Su, Z.; Xu, Q.; Luan, T.H.; Li, R. VFC-Based Cooperative UAV Computation Task Offloading for Post-disaster Rescue. In Proceedings of the IEEE INFOCOM 2020-IEEE Conference on Computer Communications, Toronto, ON, Canada, 6–9 July 2020; pp. 228–236.
4. Zhang, S.; Liu, J. Analysis and Optimization of Multiple Unmanned Aerial Vehicle-Assisted Communications in Post-Disaster Areas. *IEEE Trans. Veh. Technol.* **2018**, *67*, 12049–12060. [\[CrossRef\]](#)
5. Gao, M.; Zhang, B.; Wang, L. A Dynamic Priority Packet Scheduling Scheme for Post-disaster UAV-assisted Mobile Ad Hoc network. In Proceedings of the 2021 IEEE Wireless Communications and Networking Conference (WCNC), Nanjing, China, 29 March–1 April 2021; pp. 1–6. [\[CrossRef\]](#)

6. Saif, A.; Dimyati, K.; Noordin, K.A.; Shah, N.S.M.; Abdullah, Q.; Mukhlif, F. Unmanned Aerial Vehicles for Post-Disaster Communication Networks. In Proceedings of the 2020 IEEE 10th International Conference on System Engineering and Technology (ICSET), Shah Alam, Malaysia, 9 November 2020; pp. 273–277. [\[CrossRef\]](#)
7. Tang, H.; Wu, Q.; Xu, J.; Chen, W.; Li, B. A Novel Alternative Optimization Method for Joint Power and Trajectory Design in UAV-Enabled Wireless Network. *IEEE Trans. Veh. Technol.* **2019**, *68*, 11358–11362. [\[CrossRef\]](#)
8. Ouyang, T.; Zhou, Z.; Chen, X. Follow Me at the Edge: Mobility-Aware Dynamic Service Placement for Mobile Edge Computing. *IEEE J. Sel. Areas Commun.* **2018**, *36*, 2333–2345. [\[CrossRef\]](#)
9. Cao, P.; Liu, Y.; Yang, C.; Xie, S.; Xie, K. MEC-Driven UAV-Enabled Routine Inspection Scheme in Wind Farm Under Wind Influence. *IEEE Access* **2019**, *7*, 179252–179265. [\[CrossRef\]](#)
10. Yang, C.; Lou, W.; Liu, Y.; Xie, S. Resource Allocation for Edge Computing-Based Vehicle Platoon on Freeway: A Contract-Optimization Approach. *IEEE Trans. Veh. Technol.* **2020**, *69*, 15988–16000. [\[CrossRef\]](#)
11. Wu, Z.; Yang, Z.; Yang, C.; Lin, J.; Liu, Y.; Chen, X. Joint deployment and trajectory optimization in UAV-assisted vehicular edge computing networks. *J. Commun. Netw.* **2021**, 1–12. [\[CrossRef\]](#)
12. Li, P.; Xu, J. Fundamental Rate Limits of UAV-Enabled Multiple Access Channel With Trajectory Optimization. *IEEE Trans. Wirel. Commun.* **2020**, *19*, 458–474. [\[CrossRef\]](#)
13. Xie, L.; Xu, J.; Zhang, R. Throughput Maximization for UAV-Enabled Wireless Powered Communication Networks. *IEEE Internet Things J.* **2019**, *6*, 1690–1703. [\[CrossRef\]](#)
14. Liu, Y.; Yang, C.; Jiang, L.; Xie, S.; Zhang, Y. Intelligent Edge Computing for IoT-Based Energy Management in Smart Cities. *IEEE Netw.* **2019**, *33*, 111–117. [\[CrossRef\]](#)
15. Lv, B.; Yang, C.; Chen, X.; Yao, Z.; Yang, J. Task Offloading and Serving Handover of Vehicular Edge Computing Networks Based on Trajectory Prediction. *IEEE Access* **2021**, *9*, 130793–130804. [\[CrossRef\]](#)
16. Zhang, X.; Zhong, Y.; Liu, P.; Zhou, F.; Wang, Y. Resource Allocation for a UAV-Enabled Mobile-Edge Computing System: Computation Efficiency Maximization. *IEEE Access* **2019**, *7*, 113345–113354. [\[CrossRef\]](#)
17. Liu, Y.; Xie, S.; Zhang, Y. Cooperative Offloading and Resource Management for UAV-Enabled Mobile Edge Computing in Power IoT System. *IEEE Trans. Veh. Technol.* **2020**, *69*, 12229–12239. [\[CrossRef\]](#)
18. Zhou, F.; Wu, Y.; Hu, R.Q.; Qian, Y. Computation Rate Maximization in UAV-Enabled Wireless Powered Mobile-Edge Computing Systems. *IEEE J. Sel. Areas Commun.* **2018**, *36*, 1927–1941. [\[CrossRef\]](#)
19. Liu, Y.; Xie, S.; Yang, Q.; Zhang, Y. Joint Computation Offloading and Demand Response Management in Mobile Edge Network With Renewable Energy Sources. *IEEE Trans. Veh. Technol.* **2020**, *69*, 15720–15730. [\[CrossRef\]](#)
20. Liu, Y.; Xiong, K.; Ni, Q.; Fan, P.; Letaief, K.B. UAV-Assisted Wireless Powered Cooperative Mobile Edge Computing: Joint Offloading, CPU Control, and Trajectory Optimization. *IEEE Internet Things J.* **2020**, *7*, 2777–2790. [\[CrossRef\]](#)
21. Liu, Y.; Qiu, M.; Hu, J.; Yu, H. Incentive UAV-Enabled Mobile Edge Computing Based on Microwave Power Transmission. *IEEE Access* **2020**, *8*, 28584–28593. [\[CrossRef\]](#)
22. Xie, L.; Xu, J.; Zeng, Y. Common Throughput Maximization for UAV-Enabled Interference Channel With Wireless Powered Communications. *IEEE Trans. Commun.* **2020**, *68*, 3197–3212. [\[CrossRef\]](#)
23. Zhang, S.; Zhang, H.; Di, B.; Song, L. Cellular UAV-to-X Communications: Design and Optimization for Multi-UAV Networks. *IEEE Trans. Wirel. Commun.* **2019**, *18*, 1346–1359. [\[CrossRef\]](#)
24. Zhong, W.; Xie, K.; Liu, Y.; Yang, C.; Xie, S.; Zhang, Y. Multi-Resource Allocation of Shared Energy Storage: A Distributed Combinatorial Auction Approach. *IEEE Trans. Smart Grid* **2020**, *11*, 4105–4115. [\[CrossRef\]](#)
25. Zhong, W.; Xie, K.; Liu, Y.; Xie, S.; Xie, L. Chance Constrained Scheduling and Pricing for Multi-Service Battery Energy Storage. *IEEE Trans. Smart Grid* **2021**, *12*, 5030–5042. [\[CrossRef\]](#)
26. Zhong, W.; Xie, S.; Xie, K.; Yang, Q.; Xie, L. Cooperative P2P Energy Trading in Active Distribution Networks: An MILP-Based Nash Bargaining Solution. *IEEE Trans. Smart Grid* **2021**, *12*, 1264–1276. [\[CrossRef\]](#)
27. Gao, Y.; Tang, H.; Li, B.; Yuan, X. Robust Trajectory and Power Control for Cognitive UAV Secrecy Communication. *IEEE Access* **2020**, *8*, 49338–49352. [\[CrossRef\]](#)
28. Cui, M.; Zhang, G.; Wu, Q.; Ng, D.W.K. Robust Trajectory and Transmit Power Design for Secure UAV Communications. *IEEE Trans. Veh. Technol.* **2018**, *67*, 9042–9046. [\[CrossRef\]](#)
29. Zhou, Y.; Zhou, F.; Zhou, H.; Ng, D.W.K.; Hu, R.Q. Robust Trajectory and Transmit Power Optimization for Secure UAV-Enabled Cognitive Radio Networks. *IEEE Trans. Commun.* **2020**, *68*, 4022–4034. [\[CrossRef\]](#)
30. Yang, T.; Taghizadeh, O.; Hu, Y.; Xu, H.; Caire, G. Robust Secure UAV Communication Systems with Full-Duplex Jamming. In Proceedings of the 2021 IEEE Wireless Communications and Networking Conference (WCNC), Nanjing, China, 29 March–1 April 2021; pp. 1–6. [\[CrossRef\]](#)